Miniaturized probe using 2 axis MEMS scanner for endoscopic multiphoton excitation microscopy

Woonggyu Jung[*,1,2], Shuo Tnag[3], Tiquiang Xie[1], Daniel T. McCormick[4], Yeh-Chan Ahn[1], Jianping Su[1,2], Ivan V. Tomov[1], Tatiana B. Krasieva[1], Bruce J. Tromberg[1,2], Zhongping Chen[1,2]

[1]Beckman Laser Institute, University of California, Irvine, CA, USA
[2]Department of Biomedical Engineering, University of California, Irvine, CA, USA
[3]Department of Electrical and Computer Engineering, University of British Columbia, Canada
[4]Advanced MEMS, Berkeley, CA, USA

ABSTRACT

The practical limitation of *in vivo* multiphoton excitation microscopy (MPM) is the lack of a compact and flexible probe. Most MPM depends on the bench-top microscope, which prohibits expansion of *in vivo* application. In this study, we introduced a miniaturized MPM probe using a microelectromechanical system (MEMS) scanning mirror and a double-clad photonic crystal fiber (DCPCF). Benefits from both a MEMS mirror and a DCPCF overcome current obstacles for probe development, such as size reduction, rapid scanning, efficient delivery of short pulses, and high collection rate of fluorescent signals. In this study, the completed probe was 1 cm in outer diameter and 14 cm in length. The probe was then integrated to the MPM system and used to image fluorescent beads, paper and biological specimens.

Keywords: Multiphoton excitation microscopy, MEMS scanning mirror, Double-clad photonic crystal fiber

1. INTRODUCTION

Multiphoton microscopy is a fluorescence imaging technique using excitation of fluorophores within specimens. It usually provides imaging and monitoring of morphological changes in living tissue at the cellular level [1,2]. Multiphoton excitation occurs only at the focus of the microscope objective, which minimizes photobleaching and photodamage. The advantages of MPM also include intrinsic sectioning capability due to nonlinear interaction and deep tissue imaging by near-infrared light. These combined benefits provide broad applications for a noninvasive diagnostic tool of biological specimens. In spite of its significant performance and mature technique development, there are practical limitations, because it is dependent on the bench-top microscope. Thus, it restricts many *in vivo* applications. For this reason, several researchers have tried to develop a compact MPM probe [3-8]. In the design and fabrication of such a probe, there are key challenges; (1) a compact scanning mechanism, (2) efficient delivery of an ultrashort pulse, (3) collection of fluorescence signals, (4) optimal micro optics design, (5) integration and packaging.

Our MPM probe used a MEMS scanning mirror and a DCPCF to satisfy these requirements. Recently, a MEMS scanning mirror has been widely used to realize compact imaging probes [7-10]. MEMS technology has many advantages including rapid scanning, small size, high reliability, mass production, and flexibility in scanning pattern capabilities. The use of a MEMS scanning mirror in an MPM probe provides not only a reduction of probe size but also rapid data acquisition for a real time, *in vivo* clinical study. Up to now, most common scanning methods of a portable MPM probe were based on the use of a pair of galvanometers or a piezoelectric actuator at the resonance frequency. These methods give high speed scanning but are limited by either the reduction of the size or the control of the scanning speed. Thus, the MEMS scanning mirror is superior to current scanning mechanism.

To date, the major obstacle in developing an MPM probe is how to deliver efficiently the ultrashort pulsed light and collect fluorescence signals from samples. The use of single/multi mode fibers has been used as an alternative means for the conventional bulk optics of MPM. However, there is a trade-off between excitation and collection efficiency. The single mode fiber (SMF) has a higher excitation rate than the multimode fiber, but has a lower collection rate [11,12]. In

Endoscopic Microscopy III, edited by Guillermo J. Tearney, Thomas D. Wang,
Proc. of SPIE Vol. 6851, 68510D, (2008) · 1605-7422/08/$18 · doi: 10.1117/12.764356

addition, the shape and spectrum of an intense short pulse though the SMF core are degraded by a nonlinear process known as self phase modulation (SPM). The recent advent of DCPCF overcomes this limitation [8,12]. The structure of the DCPCF consists of a large core surrounded by inner and outer cladding. The excitation light propagates through the single mode core, and the collected fluorescence light guides back through the cladding supporting multimode. The DCPCF not only enhances the sensitivity but also minimizes the SPM because the relatively large core can significantly reduce the power density of short pulse light. In this study, we merge the benefits of the MEMS scanning mirror and the DCPCF to realize a completed probe.

2. EXPERIMENTS

2.1 MEMS mirror and bench-top testing

In a preliminary experiment, we realized a bench-top MPM probe system (Fig. 1). The system consists of a DCPCF fiber, a MEMS scanning mirror, and lenses. The DCPCF (Crystal Fibre A/S) we used in this work has a core diameter of 16 μm and an inner cladding with a diameter of 163 μm. A The structure and scanning mechanism of a MEMS mirror is very similar to our previous works [9,10]. Our MEMS scanning actuator is based on a monolithic, single crystal silicon, two-dimensional, gimbal-less, vertical comb-driven structure employing electrostatic forces for actuation [13]. The devices were designed and realized in a self-aligned DRIE fabrication process utilizing a silicon on insulator (SOI) wafer. The mirrors were fabricated in a separate SOI process and later bonded to the actuator allowing the actuator and mirror to be independently optimized. The mirror apertures were metalized low-inertia SCS structures using a thinned mirror plate (2-5 μm), thick stiffening trusses (~25 μm) and a tall standoff pedestal (~120 μm). The device employed in this particular study had a 2 mm diameter mirror and exhibited x- and y-axis resonant frequencies of 1.26 kHz and 780 Hz, respectively. The scanning angle of each axis was 14°. Fig. 1A presents an image of the diced 2 mm MEMS mirror.

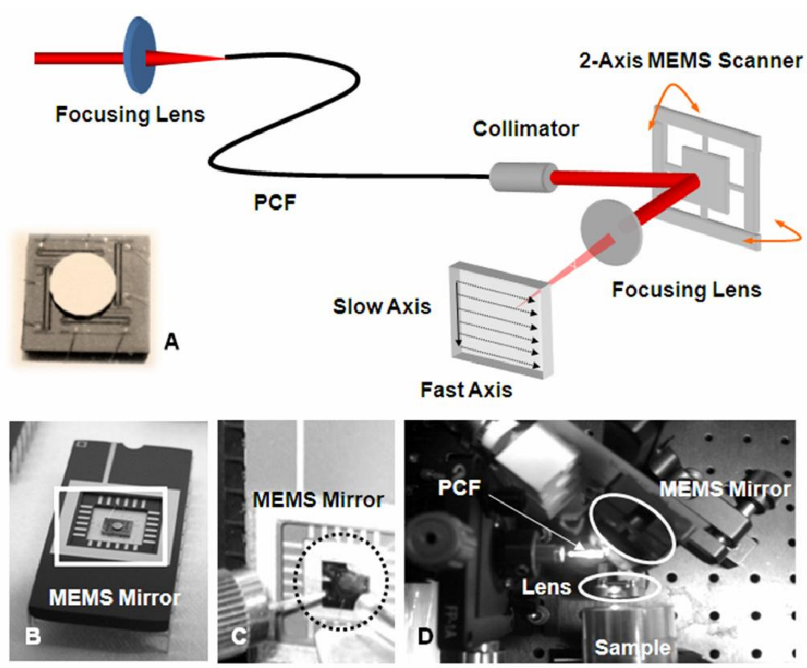

Figure 1. Schematic of bench-top MPM probe system using DCPCF and chip based MEMS scanning mirror. 2D image was acquired by combination of fast transverse scanning and slow longitudinal scanning; A. Photograph of diced two-axis MEMS mirror. The 2 mm mirror was fabricated in a separate process for quality control and later bonded to the actuator; B. Photograph of two-axis MEMS scanning mirror packaged in 24 pin DIP for characterization and bench-top testing; C,D. Photograph of experimental setup.

A 2mm MEMS mirror initially was packaged in 24 pin DIP as shown fig. 2B. Then the other optical components, such as gradient index (GRIN) lens, DCPCF, MEMS mirror, were aligned in free space (figs. 2C and D).

This setup characterized various scan patterns with a visible light source to demonstrate the flexibility of the MEMS scanner as well as optical designs described in the next section.

2.2 Optic designs of probe

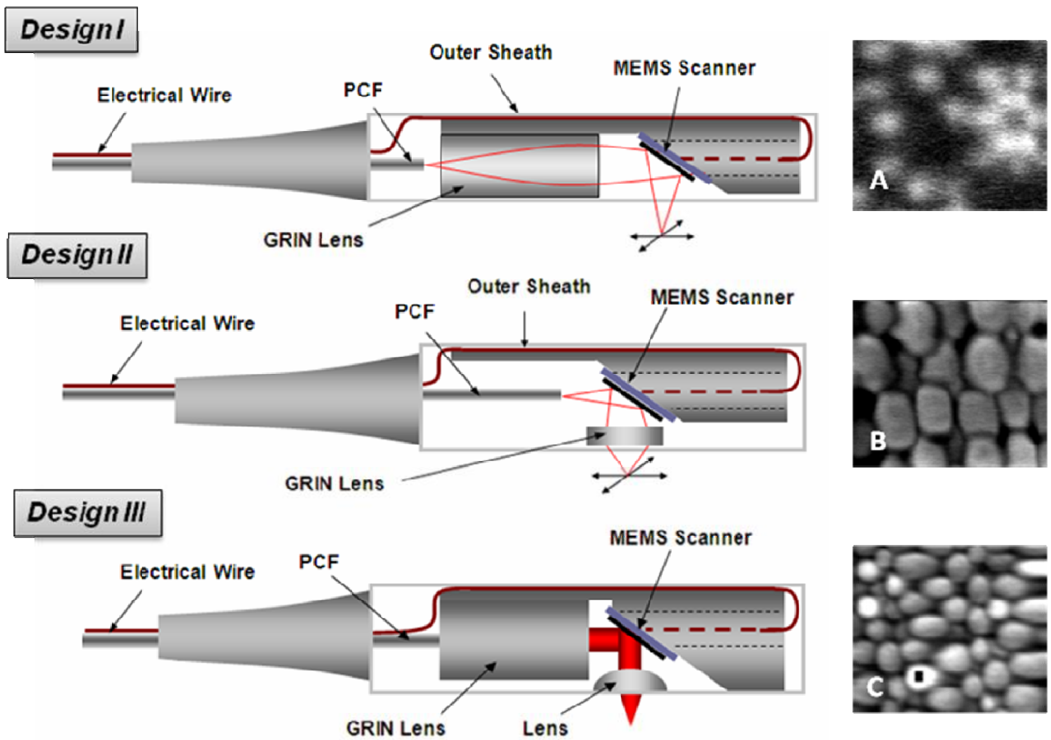

Figure 2. Various optical designs of probe and images. Three different designs were considered using different combinations of DCPCF, GRIN lens, and MEMS scanning mirror; *Design I.* PCF & GRIN lens (0.29 pitch, 0.64 NA) & MEMS mirror; *Design II.* PCF & MEMS mirror & GRIN lens (0.23 pitch, 0.64 NA); *Design III.* PCF & GRIN lens (0.22 pitch) & MEMS mirror & Aspheric lens (0.62 NA, 4.03 mm focal length). In bench-top testing, a 2 m PCF fiber was used. All images show 20 micron fluorescent beads by the different optical designs and same scanning angle of the MEMS mirror.

The optics of the probe could be varied by the selection and arrangement of components, such as DCPCF, GRIN lens, MEMS mirror. Fig. 2 shows the different designs that we considered. Design I is the simplest case that could be realized for an endoscopic probe. This is a very similar concept with an our previous 3D endoscopic optical coherence tomography probe [10]. It has the advantage of relatively easy alignment and packaging as well as size efficiency. However, it requires a lens with a long working distance in order for the beam to escape from the packaging. It usually produces less resolution at the focal point. In our experiment, we used a 0.29 pitch GRIN lens at 800nm had a 5.5 mm working distance with calculation. A corresponding image with design I visualizes 20 um beads (fig. 2A). Design II could increase the resolution due to the GRIN lens location after the MEMS mirror. Thus, less working distance required and overcomes the resolution problem of Design I. With the second design, we also imaged 20 um beads (fig. 2B), which shows improved resolution over design I. Even though design II could be applicable for a miniaturized probe, it is difficult to package and there is a limited scanning area due to a small diameter of the GRIN lens for the focusing lens. The last design originated from design II. The difference compared between a design II and III is use of the collimated beam and aspheric lens for focusing instead of the GRIN lens. The span between GRIN lens and DCPCF was adjusted for beam collimating which prohibited the divergence of incident light on the MEMS mirror. This effect induces a large fill factor on the MEMS mirror and increases the imaging area with the large diameter of the lens. The focusing lens had the same length as the GRIN lens in design II but a large diameter. Thus, the probe could be realized the same size as design II and easily packaged. In addition, the higher NA of the focusing lens produced a higher resolution image. Fig. 3C shows the large scanning area and resolution improvement.

2.3 Completed MPM and packaging

The Ti:sappihire laser was first coupled with a 1 m DCPCF and guided to the core. In order to generate the collimated beam, the DCPCF and a 1.8 mm GRIN lens (0.22 pitch, NA=0.6) were then aligned in the transparent tubing. The optimal collimating beam was monitored by the adjustment of the span between the DCPCF and GRIN lens and glued with UV curing adhesive (Fig. 3A). The assembled pigtailed GRIN lens was inserted into a 2.5 mm diameter metal tube, aligned in the center and glued again in order to protect from breakage. For integration and packaging, all mounts, alignment bench, and housings were fabricated. The MEMS scanner was mounted on one end of a 45° platform of the alignment bench to serve as a support for the mirror die; sufficient material remained on the tube walls to maintain mechanical rigidity and structural integrity. Wires with a diameter of 200 μm were then passed through the access holes and secured in place with epoxy; the surface of the wires were then planarized and served as bonding pads. The tail of the wires were bent back and run through a channel along the bottom of the alignment bench. A pig-tailed GRIN lens was mounted on the other end of alignment bench and temporarily held in place while the MEMS mirror was positioned. The course alignment of the components utilizing a stereoscope and a visible laser were coupled into the pigtailed GRIN lens. The mirror was then fixed in place, and the wirebond connections were made between the MEMS die and alignment bench. The assembled device was covered by a transparent inner sheet, inserted into the steel inner housing and glued with epoxy as depicted in Fig. 3B. The inner housing was then inserted inside a prepared steel outer housing. Finally, a focusing lens (D=5 mm) was placed on the mount and aligned on the center of the beam from the MEMS mirror. For convenience of alignment, a railed notches were made in both the steel inner and outer housing. The completed probe looks like a submarine as shown in Fig. 3C. The outer diameter and length was 1 cm and 14 cm, respectively. The diameter of the lens mount was 7 mm and the length varied from 6 mm to 1.5 cm.

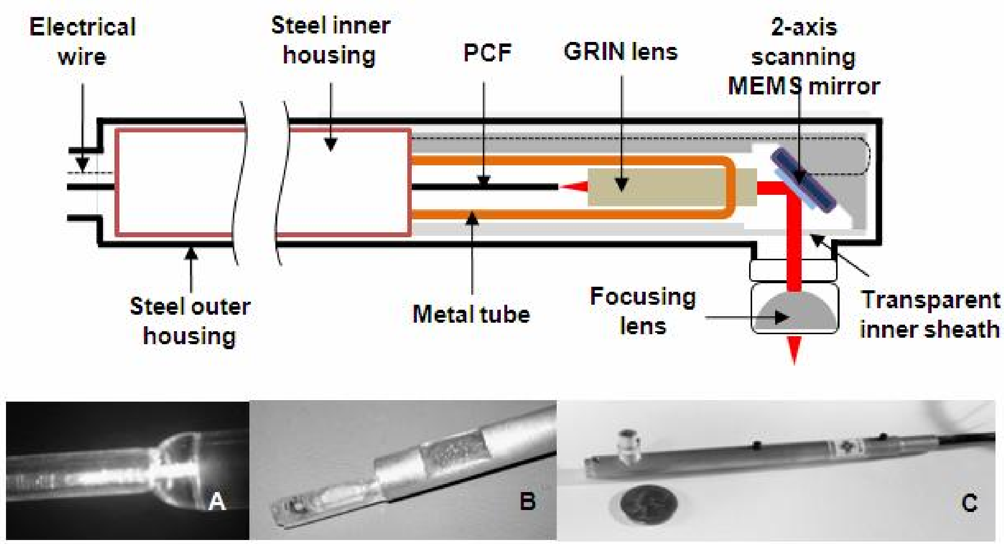

Figure 3. Schematic and photographs of the completed MPM probe; A. Photograph of GRIN lens assembled with DCPCF; B. MEMS mirror and pigtailed GRIN lens were mounted to home-made packaging. Photograph shows the before integration with outer steel housing; C. Photograph of completed probe. Submarine shaped probe compared for size to a U.S. quarter coin. The outer diameter and length of the probe were 1 cm and 14 cm, respectively. The notch on the rail between inner and outer housing provides flexible alignment. The distance of the lens mount from the steel outer housing is adjustable.

2.4 MPM system using miniaturized probe

The completed probe was incorporated with the MPM system as presented in Fig. 4A. TI:sapphire laser provided the excitation source at a wavelength of 790 nm with a bandwidth of 45 nm. The average laser output power was 450 mW at 76 MHz. A Femtosecond pulse from the laser was negatively prechirped by grating pairs in order to compensate for positive dispersion due to beam propagation through the core of the DCPCF. To confirm dispersion compensation, the pulse duration was measured before and after propagation through the MPM probe. Fig. 4(A and B) show the pulse width from the direct laser and after compensation. The 190 fs pulse (Fig. 4A) from the laser was broadened by more than 2 ps, which was compensated as 260 fs (Fig. 4B). The beam was then launched into the DCPCF using a coupling lens (NA= 0.1, 5×) and reflected by a MEMS mirror. An aspheric lens (f=4.03, NA= 0.62) was used to focus the scanned beam from the MEMS mirror. The fluorescence signal emitted by the sample was collected back through the cladding of the DCPCF and separated from the input beam with a dichroic mirror. The fluorescence signal was then filtered by the short pass filter (cutoff wavelength: 650 nm) and directed toward a photomultiplier tube (PMT). The signal from the PMT was amplified, digitized and visualized as an image.

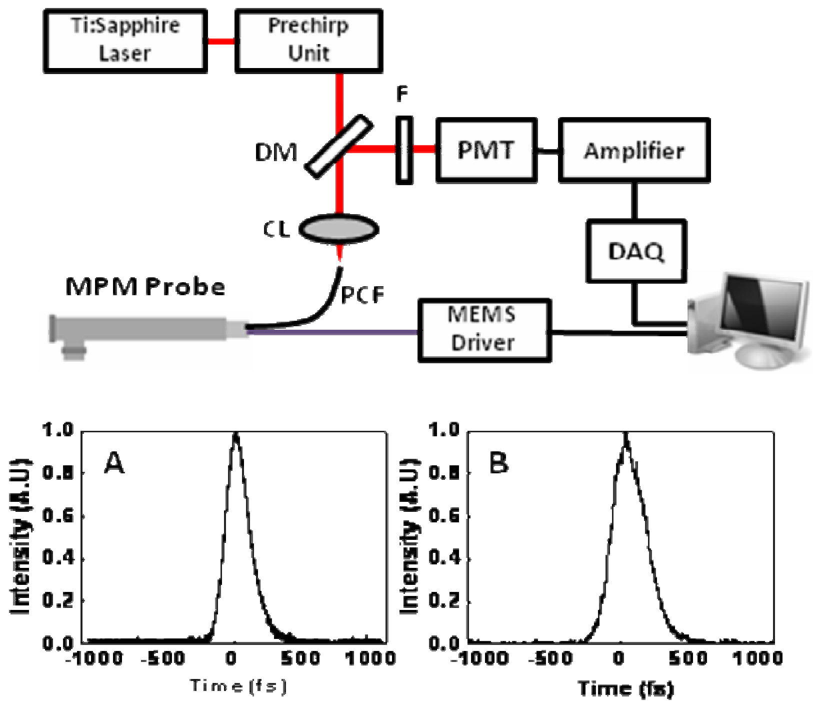

Figure 4. Schematic of MPM incorporated with probe. In order to compensate the positive dispersion due to 1 m DCPCF, prechirping units using grating pair were used. MEMS mirror was controlled by the sychnonized signal generated from a computer: (A) Measurement of laser pulse duration (190 fs); (B) Pulse duration after prechirping units. Broadened pulse (more than 2 ps) was minimized up to 260 fs.

3. RESULTS

Fig. 5A shows an image of 6 μm fluorescence beads. The image consists of 512 by 512 pixels at a scanning rate of 10 Hz. The excitation power delivered to the sample was 15 mW through the core of the DCPCF. Figure 5B depicts an MPM image of a piece of paper. Fluorescent whitening agents are commonly added to paper during manufacture to impart whiteness and brightness. The paper containing fluorescent whitening agents generates a high fluorescence signal. The acquired image visualizes the grid structure of the paper with detailed fibers. To prove the imaging capability using the developed probe for clinical study, we imaged *in vitro* articular cartilage and bone (Fig. 5C-E). Articular cartilage contains chondrocytes which vary in number, a shape, an orientation at different location. Figure 3C shows the different feature of chondrocytes along the depths of a superficial region. Finally, the shape of the chondrocyte becomes circle at the deep zone as presented in Fig. 5D. The center spot indicates the nuclei of the chondrocyte. The performance of our system was also compared to a commercial MPM system. The specs of the commercial MPM were setup with the same values as our developed system: optical power, wavelength, NA of objective lens, scanning rate. Bone tissue beneath the articular cartilage was imaged with both systems (Fig. 5E,F). The images obtained from our system and the commercial system were similar and correlated very well.

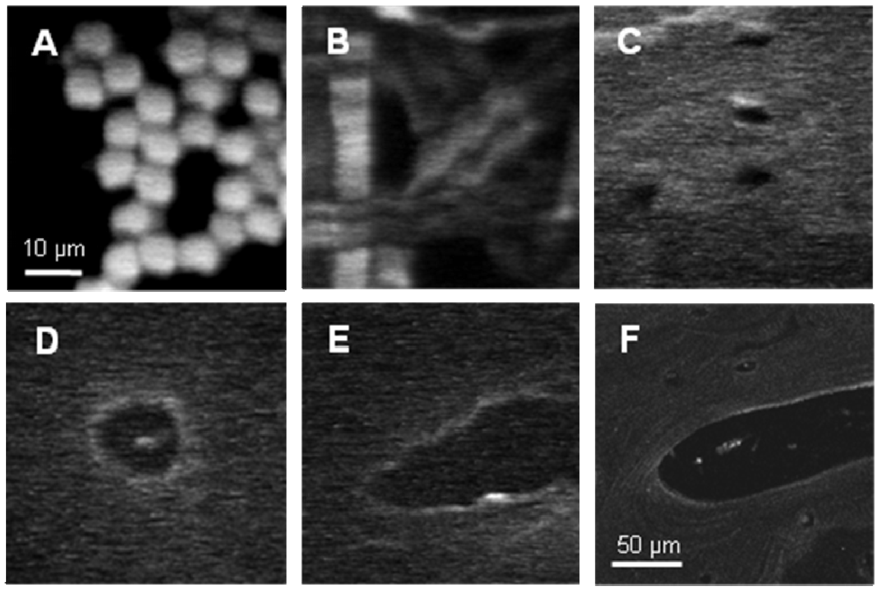

Figure 5. In vitro MPM images using a compact probe. The excitation power on the sample was 15 mW. (A) Image of 6 μm fluorescent beads. (B) Image of paper. Each fiber is clearly visualized. (C) Images of chondrocytes in a superficial articular cartilage. (D) Image of chondrocytes in the deep zone. (E) Image of bone by the MPM system using the probe. (F) Image of bone by commercial MPM system. In order to compare the performance of the probe MPM system over standard MPM system, similar optical conditions were assigned such as optical power, wavelength, NA of objective lens, and scanning rate. The images acquired by the probe MPM system and standard MPM were of similar quality.

4. CONCLUSION

In summary, a portable MPM probe using a MEMS mirror was designed and constructed. By using MEMS mirror with conventional scanning methodology, we were able to deveople the compact probe. The probe also allows efficient delivery of a short pulse laser and collection of fluorescent signals. With these advantages, the probe was integrated into an MPM system and provided high resolution images comparable to a commercial system. The capability of the current device could function as an endoscopic tool by means of optimal micro optics and further reduction in packaging. Such a compact probe may expand the application of MPM as a promising device for high resolution diagnostic imaging.

ACKNOWLEDGMENTS

Advanced MEMS is gratefully acknowledged for providing the probe and control system. This work was supported by research grants from the National Science Foundation (BES-86924), National Institutes of Health (EB-00255, NCI-91717, RR-01192), and the Air Force Office of Scientific Research (FA9550-04-1-0101). Institutional support from the Beckman Laser Institute Endowment is also acknowledged. Z. Chen's address is z2chen@uci.edu.

REFERENCES

[1] W. Denk, J. H. Strickler, and W. W. Webb, "Two-photon laser scanning fluorescence microscopy," Science **248**, 73 (1990).
[2] W. R. Zipfel, R. M. Williams and W. W. Webb, "Nonlinear magic: multiphoton microscopy in the biosciences," Nat. Biotechnol. **21**, 1369 (2003)
[3] F. Helmchen, M. S. Fee, D. W. Tank and W. Denk, "A miniature head-mounted two-photon microscope: High-resolution brain imaging in freely moving animals," Neuron **31**, 903 (2001).

[4] J. C. Jung and M. J. Schnitzer, “Multiphoton endoscopy,” Opt. Lett. **28**, 902 (2003).

[5] B. A. Flusberg, J. C. Jung, E. D. Cocker, E. P. Anderson, and M. J. Schnitzer, “In vivo brain imaging using a portable 3.9 gram two-photon fluorescence microendoscope,” Opt. Lett. **30**, 2272 (2005).

[6] M. T. Myaing, D. J. MacDonald, and X. Li, “Fiber-optic scanning two-photon fluorescence endoscope,” Opt. Lett. **31**, 1076 (2006).

[7] W. Piyawattanametha, R. P. J. Barretto, T. H. Ko, B. A. Flusberg, E. D. Cocker, H. Ra, D. Lee, O. Solgaard, and M. J. Schnitzer, “Fast-scanning two-photon fluorescence imaging based on a microelectromechanical systems two-dimensional scanning mirror,” Opt. Lett. **31**, 2018 (2006)

[8] L. Fu, A. Jain, C. Cranfield, H. Xie, and M. Gu, “three-dimensional nonlinear optical endoscopy,” J. Biomed. Opt. **12**, 040501-1 (2007).

[9] W. Jung, D. T. McCormick, J. Zhang, L. Wang, N. C. Tien, and Z. Chen, “Three-dimensional endoscopic optical coherence tomography by use of a two-axis microelectromechanical scanning mirror,” Appl. Phys. Lett. **88**, 163901 (2006).

[10] W. Jung, D. T. McCormick, Y. Ahn, A. Sepehr, M. Brenner, B. Wong, N. C. Tien, and Z. Chen, “In vivo three-dimensional spectral domain endoscopic optical coherence tomography using a microelectromechanical system mirror,” Opt. Lett. **32**, 3239 (2007).

[11] J. Y. Ye, M. T. Myaing, T. B. Norris, T. Thomas, and J. Baker, Jr, Biosensing based on two-photon fluorescence measurements through optical fibers,” Opt. Lett. **27**, 1412 (2002).

[12] M. T. Myaing, J. Y. Ye, T. B. Norris, T. Thomas, J. R. Baker, Jr., W. J. Wadsworth, G. Bouwmans, J. C. Knight, and P. St. J. Russell, “Enhanced two-photon biosensing with double-clad photonic crystal fibers,” Opt. Lett. **28**, 1224 (2003).

[13] V. Milanović, G. A. Matus, and D. T. McCormick, “Gimbal-less monolithic silicon actuators for tip-tilt-piston micromirror applications”, IEEE. J. STQE. **10**, 462 (2004).